arXiv:1512.08633v1 [physics.plasm-ph] 29 Dec 2015

Solitary structures with ion and electron thermal anisotropy

Murchana Khusroo and Madhurjya P Bora

Physics Department, Gauhati University, Guwahati 781014, India.

E-mail: mpbora@gauhati.ac.in

April 2015

Abstract. Formation of electrostatic solitary structures are analysed for a magnetised plasma with ion and electron thermal anisotropies. The ion thermal anisotropy is modelled with the help of the Chew-Goldberger-Low (CGL) double adiabatic equations of state while the electrons are treated as inertia-less species with an anisotropic bi-Maxwellian velocity distribution function. A negative electron thermal anisotropy ($T_{e\perp}/T_e\| > 1$) is found to help form large amplitude solitary structures which are in agreement with observational data.

1. Introduction

Solitary structures, commonly known as electrostatic solitary waves (ESWs) or Solitons are frequently observed in the near-earth plasmas and in the boundary layers of the earth's magnetosphere [1, 2]. A soliton is a single wave pulse which is generated due to accumulation of electron density at a particular region. When there is an inhomogeneity of electrons (or ions) due to the evolution of nonlinear perturbation, it results in the formation of a potential structure at that specific region, and henceforth an electric field is generated which is in fact detected by the spacecraft in the form of a bipolar pulse [2, 3, 4]. Theoretical and observational studies have indicated that these ESWs are basically potential structures and weak double layers [5].

In the recent years many physical models have been put forward by various authors trying to give a correct explanation for the existence of these solitary structures [6, 7, 8, 9, 10, 11]. In a complex plasmas such as planetary magnetosphere, various physical effects play crucial roles in formation of these structures. The ambient magnetic field in a plasma may lead to this pressure anisotropy due to disparate time scales in parallel and perpendicular directions of the magnetic field when Coulomb collisions are sufficiently weak. Many astrophysical plasmas are magnetised and can be considered almost collisionless where thermal anisotropy is an important factor [12, 13]. In near-earth plasmas, field-aligned electron anisotropies have been found on auroral and magnetospheric plasmas in both high and low altitudes [15, 16].

We note that that a full-blown analyses of solitary waves with self-consistent perturbation of the magnetic field can be very complicated indeed [17]. Various authors have studied the effect of pressure anisotropy on formation of nonlinear structures in electron-positron-ion (epi) plasmas [18], dusty plasmas [19, 20, 21], and plasmas with κ-distributed electrons [22]. We, in this work, have considered formation of these ion-acoustic ESWs in the presence of both ion and electron thermal anisotropy, in the presence of a background magnetic field. In Section 2, we have presented the plasma model for the formation of these ESWs in a magnetoplasma with ion pressure anisotropy. In Section 3, we describe a general procedure for reducing the mathematical equations to study these solitary structures. In Section 4, we incorporate the electron thermal anisotropy through a bi-Maxwellian velocity distribution function. In Section 5, we have formulated the pseudo potential analysis and compared our theoretical results with available observational data. Finally in Section 6, we summarise our results and conclusions.

2. The plasma model

The basic model of our plasma is represented by the following MHD equations,

$$\frac{\partial n}{\partial t} + \nabla.(n\boldsymbol{v}) = 0, \tag{1}$$

$$\frac{d\boldsymbol{v}}{dt} = -\frac{e}{m_i}\nabla\phi - \frac{1}{m_i n}\nabla\cdot\boldsymbol{p} + (\boldsymbol{v}\times\boldsymbol{\Omega}_i), \tag{2}$$

which are ion continuity and momentum equations where n is the ion density, $\Omega_i = eB/(m_i c)$ is the ion gyro-frequency, and $\boldsymbol{p}$ is the anisotropic pressure tensor,

$$\boldsymbol{p} = p_\perp(\boldsymbol{I} - \boldsymbol{bb}) + p_\parallel \boldsymbol{bb}, \tag{3}$$

with $\boldsymbol{I}$ as the unit dyadic and $\boldsymbol{b} = \boldsymbol{B}/B$ is the unit vector along the field line. The other symbols have their usual meanings. Electrons are assumed to be Boltzmannian. We also invoke the quasi-neutrality condition

$$n = n_e = F(\phi), \tag{4}$$

where F is a function of plasma potential ϕ. The ion thermal-anisotropy is assumed to be described the CGL double adiabatic laws [24],

$$\frac{d}{dt}\left(\frac{p_\perp}{\rho B}\right) = 0, \tag{5}$$

$$\frac{d}{dt}\left(\frac{p_\parallel B^2}{\rho^3}\right) = 0. \tag{6}$$

We assume the external magnetic field $\boldsymbol{B}$ is in the $\hat{\boldsymbol{z}}$ direction and plasma approximation is assumed all throughout. The application of plasma approximation, in general, implies that the time scale of perturbation is large enough so that variation of electric potential ϕ due to electrons and ions in space, can be thought to be smeared out and the scale length over which ϕ varies, is considerably larger than the Debye screening length λ_D. For our

intended parameter regime of magnetosphere of the earth including auroral regions, this can be justified, where solitary structures of the order of $\sim 10\lambda_D$ are observed in the auroral regions [25, 26, 27, 28].

2.1. CGL anisotropy

We note that the double adiabatic equations (CGL theory) [24] is rather restrictive in its application as the system *must* vary sufficiently slowly along the field lines so that particles with different behaviour at two different points, even along the lines of force, have only little communication [29]. However, we should note that the CGL equations are actually a subset of a more general polybaric pressure equations [30],

$$p_\perp \propto N^\gamma B^\kappa, \tag{7}$$

$$p_\parallel/p_\perp \propto N^{\gamma_a} B^{\kappa_a}. \tag{8}$$

The CGL equations can be recovered for $\gamma = \kappa = 1$, and $\gamma_a = 2, \kappa_a = -3$. Measurements from Cluster series of spacecrafts in the earth's magnetosphere has indicated that the ion anisotropy can be well modelled by Eqs.(7,8) [31, 32] for different values of the parameters $\gamma, \gamma_a, \kappa, \kappa_a$. However, our prime objective in this paper has been to incorporate the ion and electron thermal anisotropies as a *proof of concept* rather than use it to fully explain observationally obtained experimental data. We also note that space plasmas including geomagnetic and auroral plasmas are diverse enough to call for different physical effects to be incorporated in the theory and in a restricted parameter regime, the CGL theory is actually found to largely agree with observational data in solar wind plasmas [33].

3. Reduction of equations

We now describe a general procedure for reducing Eqs.(1-6) for nonlinear perturbation [11]. We assume an arbitrary electrostatic perturbation in time and space and define a co-moving co-ordinate $\eta = l_x x + l_z z - v_M t$, where $l_{x,z}$ are direction co-sines and thus defined by the relation $l_x^2 + l_z^2 = 1$ and v_M is the velocity of the nonlinear wave. Far away from the perturbation, we assume everything to be stationary and define the boundary conditions : $\eta \to \infty$, $n \to n_0$, $\phi \to 0$, and $v \to 0$. Without any loss of generality, we can assume that the physical quantities to be constant along the $\hat{\boldsymbol{y}}$ direction. Note that in the scaled coordinates, we have,

$$\left.\begin{aligned} \frac{\partial}{\partial t} &\equiv \frac{\partial \eta}{\partial t}\frac{\partial}{\partial \eta} \equiv -v_M \frac{\partial}{\partial \eta}, \\ \frac{\partial}{\partial x} &\equiv \frac{\partial \eta}{\partial x}\frac{\partial}{\partial \eta} \equiv l_x \frac{\partial}{\partial \eta}, \\ \frac{\partial}{\partial z} &\equiv \frac{\partial \eta}{\partial z}\frac{\partial}{\partial \eta} \equiv l_z \frac{\partial}{\partial \eta}. \end{aligned}\right\} \tag{9}$$

From the continuity equation we get

$$l_x v_x + l_z v_z - v_M = -v_M \frac{n_0}{n}, \tag{10}$$

From the x, y, and z components of the momentum equation, we get,

$$-v_M \frac{n_0}{n} v_x' = -l_x \left[g(n) + h_\perp(n)\right] + v_y \Omega_i, \tag{11}$$

$$-v_M \frac{n_0}{n} v_y' = -v_x \Omega_i, \tag{12}$$

$$-v_M \frac{n_0}{n} v_z' = -l_z \left[g(n) + h_\parallel(n)\right], \tag{13}$$

where

$$g(n) = \frac{e}{m_i}\phi', \tag{14}$$

$$h_\perp(n) = \frac{p_{\perp 0}}{m_i n n_0} n', \tag{15}$$

$$h_\parallel(n) = \frac{3 p_{\parallel 0} n}{m_i n_0^3} n', \tag{16}$$

and $(')$ denotes derivative with respect to η.

At this point, we would like to introduce the normalisation that we are going to use. The ion density n is normalised to its equilibrium density n_0, $p_{\parallel,\perp}$ to $n_0 T_{\parallel 0,\perp 0}$, velocities to the ion-sound velocity $v_s = \sqrt{T_{e0}/m_i}$, potential to T_{e0}/e, length to the ratio v_s/Ω, and time to Ω^{-1}. The ratio of the ion temperature to the electron temperature is denoted by $\sigma = T_0/T_{e0}$. The normalised equations are then given by,

$$l_x v_x + l_z v_z - v_M = -\frac{v_M}{n}, \tag{17}$$

$$-\frac{v_M}{n} v_x' = -l_x \left[g(n) + h_\perp(n)\right] + v_y, \tag{18}$$

$$-\frac{v_M}{n} v_y' = -v_x, \tag{19}$$

$$-\frac{v_M}{n} v_z' = -l_z \left[g(n) + h_\parallel(n)\right]. \tag{20}$$

Differentiating Eqs.(18) and (20) with respect to η we get,

$$-\frac{v_M}{n} v_x'' + \frac{v_M n'}{n^2} v_x' = \frac{n}{v_M} v_x - l_x \left[g'(n) + h_\perp'(n)\right], \tag{21}$$

$$-\frac{v_M}{n} v_z'' + \frac{v_M n'}{n^2} v_z' = -l_z \left[g'(n) + h_\parallel'(n)\right], \tag{22}$$

where we have substituted the value of v_y' from Eq.(19). By differentiating Eq.(17), successively with respect to η, we get,

$$l_x v_x' + l_z v_z' = \frac{v_M n'}{n^2}, \tag{23}$$

$$l_x v_x'' + l_z v_z'' = -v_M \left(\frac{2n'^2}{n^3} - \frac{n''}{n^2}\right). \tag{24}$$

Using Eqs.(21-25), we get,

$$g'(n) + \frac{v_M^2 n'^2}{n^4} + l_z^2 h'_{\parallel}(n) + l_x^2 h'_{\perp}(n) = \frac{-v_M + n v_M - n l_z v_z}{v_M} - \frac{v_M^2}{n}\left(\frac{2n'^2}{n^3} - \frac{n''}{n^2}\right), \tag{25}$$

where we have used the condition $l_x^2 + l_z^2 = 1$ and substituted the value of v_x from Eq.(17). Eq.(22) can be integrated to have

$$v_z = c_1 + \frac{l_z}{v_M}\int n\left[g(n) + h_{\parallel}(n)\right]\, d\eta \tag{26}$$

where c_1 is the constant of integration to be evaluated by imposing the boundary conditions. So, finally, using Eqs.(26), from Eq.(25), we arrive at a single nonlinear second order differential equation for the system,

$$\begin{aligned} 1 + g'(n) = & -\frac{3v_M^2 n'^2}{n^4} - l_z^2 h'_{\parallel}(n) - l_x^2 h'_{\perp}(n) \\ & + \frac{n}{v_M^2}\left\{v_M(v_M - c_1 l_z) - l_z^2 \int n\left[g(n) + h_{\parallel}(n)\right]\, d\eta\right\} \\ & + \frac{v_M^2 n''}{n^3}. \end{aligned} \tag{27}$$

With specific electron distribution and together with plasma approximation, Eq.(27) can be written in a generic form as,

$$\alpha(n)n'' + \beta(n)n'^2 + \zeta(n) = 0, \tag{28}$$

where $\alpha(n), \beta(n)$, and $\zeta(n)$ are arbitrary functions of n. Eq.(27) can be re-cast as,

$$\lambda(n)\frac{d^2G(n)}{d\eta^2} + \zeta(n) = 0, \tag{29}$$

where $\lambda(n)$ and $G(n)$ are functions of n, to be determined. The Sagdeev potential $V(n)$ can now be written in terms of $G(n)$ as,

$$V(n) = -\int^n \frac{\zeta(n)}{\lambda(n)} G'(n)\, dn + c_2, \tag{30}$$

where c_2 is an integration constant to be determined by imposing boundary conditions on $V(n)$.

By comparing the coefficients of n'' and n'^2 of Eqs.(28) and (29), we get,

$$\alpha = \lambda(n)\frac{dG(n)}{dn} = \lambda(n)G'(n), \tag{31}$$

$$\beta = \lambda(n)\frac{d^2G(n)}{d\eta^2} = \lambda(n)G''(n), \tag{32}$$

from which we can write Eq.(28) as,

$$\alpha(n)G''(n) - \beta(n)G'(n) = 0, \tag{33}$$

which determines $G(n)$ and in turn $\lambda(n)$.

3.1. Isotropic ion pressure

We note that for isotropic ion pressure, $p \propto \rho^\gamma$, the nonlinear equation, Eq.(27) becomes [11],

$$\begin{aligned} 1 + g'(n) = & -\frac{3v_M^2 n'^2}{n^4} - h'(n) \\ & + \frac{n}{v_M^2}\left\{ v_M(v_M - c_1 l_z) - l_z^2 \int n\left[g(n) + h(n)\right]\, d\eta \right\} \\ & + \frac{v_M^2 n''}{n^3}. \end{aligned} \tag{34}$$

The effect of ion pressure being anisotropic has a direct consequences on the limits of the Mach number, as we shall see in Sec.5.

4. Electron velocity distribution

In an weakly collisional or collisionless plasma, momenta of various species can not be effectively exchanged among the field aligned and perpendicular directions of the ambient magnetic field. This results in the anisotropic velocity distributions of the particles, say of electrons and ions. Besides, in the ion-acoustic time scale, which is of our interest in this work, electron inertia can very well be neglected. However, these two characteristics can be effectively included in the theory by considering the density of the lighter species be determined solely by an anisotropic velocity distribution, without considering the momentum balance. This situation is particularly true in case of equatorially trapped electrons in the geomagnetic mirror [34]. The anisotropic electron distribution in the geomagnetic field are experimentally detected by space born experiments as early as 1979 through the SCATHA and DE-1 spacecraft observations [35]. Electron thermal anisotropy is also observed in the auroral plasmas [36].

The particle density n for any arbitrary velocity distribution function $f(\boldsymbol{v}, \phi)$ in presence of an electrostatic potential ϕ, can be obtained from the basic principle,

$$n = \int f(\boldsymbol{v}, \phi)\, d^3v, \tag{35}$$

where the integral is over the entire velocity space. For an anisotropic distribution function in presence of a magnetic field, which we are going to consider in this work, the above relation can be written as,

$$n = \iint f\left(v_\perp^2, v_\parallel, \phi\right)\, dv_\perp^2 dv_\parallel. \tag{36}$$

We can now apply Liouvilles' theorem to find out the density of particles at any point along the magnetic field line, which basically states that the velocity distribution function in a collisionless plasma is constant along the particle trajectories i.e. along the magnetic lines of force [37, 38]. We assume that the total energy $\mathcal{E}$ and the adiabatic

invariant μ, the magnetic moment are constant throughout the particle trajectory and so, the distribution function can be entirely expressed in terms of these variables,

$$n_s = \frac{\pi B_s}{2}\left(\frac{2}{m}\right)^{3/2}\int\!\!\int \frac{f(\mathcal{E}-q\phi,\mu)}{(\mathcal{E}-q\phi_s-\mu B_s)^{1/2}}\,d\mathcal{E}\,d\mu, \tag{37}$$

where

$$\mathcal{E} = \frac{1}{2}m\left(v_\perp^2+v_\parallel^2\right)+q\phi, \tag{38}$$

$$\mu = \frac{1}{2}m\frac{v_\perp^2}{B}, \tag{39}$$

and the subscript 's' is the field-line label. However, by using the variables $(\mathcal{E},\mu)$, we have lost the distinction for the oppositely moving particles along a particular field line, which can be explicitly taken care of by using two distribution functions $f^\pm$ for particle moving along the line and opposite to it, $ds/dt \gtrless 0$ [37],

$$n_s = \frac{\pi B_s}{2}\left(\frac{2}{m}\right)^{3/2}\int_{\mu=0}^{\infty}\int_{\mathcal{E}=q\phi_s+\mu B_s}^{\infty}\frac{f^+ + f^-}{(\mathcal{E}-q\phi_s-\mu B_s)^{1/2}}\,d\mathcal{E}\,d\mu. \tag{40}$$

Assuming symmetry between the oppositely moving particles, which is especially true for trapped particles in the equatorial region of the geomagnetic sphere, we can set $f^+ = f^- = f$,

$$n_s = \pi B_s\left(\frac{2}{m}\right)^{3/2}\int_{\mu=0}^{\infty}\int_{\mathcal{E}=q\phi_s+\mu B_s}^{\infty}\frac{f(\mathcal{E}-q\phi,\mu)}{(\mathcal{E}-q\phi_s-\mu B_s)^{1/2}}\,d\mathcal{E}\,d\mu. \tag{41}$$

If we now take a position on a field line as a reference point, we can set $\phi = 0$ at that point and $n = n_0$, we can substitute $f(\mathcal{E}-q\phi,\mu) = f(\mathcal{E},\mu)$ in the above expression to obtain the density at any point along the field line with reference to the equatorial position,

$$n_s = \pi B_s\left(\frac{2}{m}\right)^{3/2}\int_{\mu=0}^{\infty}\int_{\mathcal{E}=q\phi_s+\mu B_s}^{\infty}\frac{f(\mathcal{E},\mu)}{(\mathcal{E}-q\phi_s-\mu B_s)^{1/2}}\,d\mathcal{E}\,d\mu. \tag{42}$$

Note that the reference position can be set to any convenient position.

However, a clarification, regarding the above expression of density n_s in terms of the magnetic field strength B_s, must be made. In principle, the value of B_s at a point 's' on the field line with respect to the '0' position should be dictated by experimental observations, say for example, in case of the geomagnetic field. However, when we would like to obtain the expression for electric potential ϕ_s at that position in terms of the density n_s, mathematically we would like to express the field strength $B_s \equiv B_s(\phi)$.

4.1. Bi-Maxwellian electron distribution

So far, we have expressed the dependence of electron density n_e on plasma potential ϕ with an generalised expression Eq.(4). We now assume that the electron population can be described by an anisotropic Maxwellian distribution [39],

$$f\left(v_\perp^2, v_\parallel\right) = n_0\left(\frac{m_e}{2\pi T_\perp}\right)\left(\frac{m_e}{2\pi T_\parallel}\right)^{1/2}\exp\left[-\frac{m_e}{2}\left(\frac{v_\perp^2}{T_\perp}+\frac{v_\parallel^2}{T_\parallel}\right)\right]. \tag{43}$$

As mentioned above, we set $\phi = 0$ at the reference point where $B = B_0$ and write the distribution as,

$$f(\mathcal{E}, \mu) = n_0 \left(\frac{m_e}{2\pi T_\perp}\right) \left(\frac{m_e}{2\pi T_\parallel}\right)^{1/2} \exp\left[-\frac{\mu B_0}{T_\perp} - \frac{\mathcal{E} - \mu B_0}{T_\parallel}\right]. \tag{44}$$

The normalised electron density n_e on an arbitrary position 's' on a field line with respect to that in the reference point, can now be written from Eq.(42) as,

$$n_e \equiv F(\phi) = \gamma(\phi) e^{\phi}, \tag{45}$$

where we have written $\phi \equiv \phi_s$ and substituted the electronic charge $q = -e$. The factor $\gamma(\phi)$ is given by,

$$\gamma(\phi) = \left[\frac{T_{e\perp}}{T_{e\parallel}} + \left(1 - \frac{T_{e\perp}}{T_{e\parallel}}\right) \frac{B_0}{B_s(\phi)}\right]^{-1}. \tag{46}$$

We note that Eq.(44) is a generalised case of the anisotropic bi-κ (or bi-Lorentzian) distribution,

$$f(\mathcal{E}, \mu) = \frac{n_0}{\pi^{3/2}\theta_\perp^2 \theta_\parallel} \frac{\Gamma(\kappa+1)}{\Gamma(\kappa - 1/2)} \left\{1 + \frac{2(\mathcal{E} - \mu B_0)}{m_e \kappa \theta_\parallel^2} + \frac{2\mu B_0}{m_e \kappa \theta_\perp^2}\right\}^{-1-\kappa}, \tag{47}$$

$$\theta_{\parallel,\perp}^2 = \frac{2T_{e\parallel,\perp}}{m_e} \left(\frac{2\kappa - 3}{\kappa}\right) \tag{48}$$

in the limit $\kappa \to \infty$. Various experimental observations indicate that geomagnetic plasmas can be fitted well with the κ distribution rather than Maxwellian. This is essentially true for a beam-plasma system where thermal equilibration time scale for the particles is less enough so that a full relaxation to a Maxwellian distribution can not occur during the dynamical time scale. However, auroral electrons can be well fitted with a bi-Maxwellian distribution [40, 41]. In case of solar wind plasmas also, which is basically a beam-plasma system, the electron population is found have two distinct distributions — a *core* population, which is very well modelled by a bi-Maxwellian distribution and a *halo* population with super-thermal particles described by κ distribution [42]. In view of this, we have chosen to consider a bi-Maxwellian electron population for our work in general, as we expect our results to be relevant in the auroral plasma regime. This assumption also simplifies our model without sacrificing the essential details.

5. The pseudo potential

We now assume that the quasi-neutrality condition Eq.(45) can be inverted for ϕ,

$$\phi = F^{-1}(n) \tag{49}$$

and can proceed to find out the equivalent Sagdeev potential, following the formalism outlined in Sec.2.

The density function $g(n)$ in terms of the inverse function can be written as,

$$g(n) = n' \frac{\partial}{\partial n} F^{-1}(n). \tag{50}$$

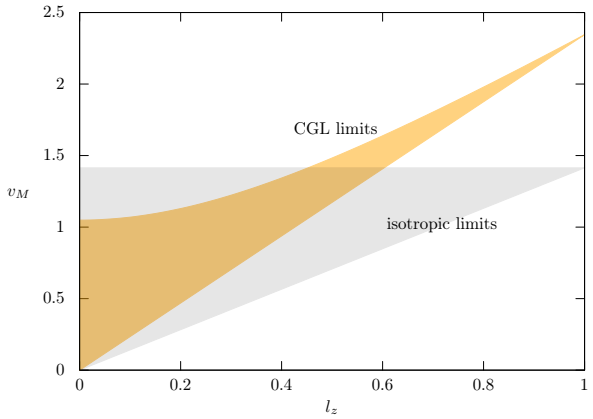

Figure 1. The limits of Mach number v_M for the CGL thermal anisotropy and isotropic pressure. The anisotropy parameters are $\sigma_\perp = 0.1, \sigma_\parallel = 1.5$ and $\sigma = 1$ for isotropic pressure.

Following the analysis (see Sec.2), the expression for the Sagdeev potential can be written as,

$$V(n) = \int^n \left[1 + \frac{n}{v_M^2}\left\{l_z^2\left(I_n + \frac{3}{4}(n^4-1)\sigma_\parallel\right) - v_M^2 - l_z^2 I_1\right\}\right] \times \left(3n^2 l_z^2\sigma_\parallel + \frac{l_x^2}{n}\sigma_\perp + \frac{\partial}{\partial n}F^{-1}(n) - \frac{v_M^2}{n^3}\right) dn + c_2, \tag{51}$$

where c_2 is the integration constant, to be found from the boundary conditions on $V(n)$. The I_n are integrals defined as,

$$I_n = \int^n n\frac{\partial}{\partial n}F^{-1}(n)\, dn. \tag{52}$$

5.1. Limiting Mach number

The limiting Mach number for formation of solitary structure can be found out by demanding the condition for local maximum for the pseudo potential $V(n)$ at $n = 1$, which can be conveniently reduced to,

$$\left[l_z^2\left(\tilde{F}_1 + 3\sigma_\parallel\right) - v_M^2\right]\left[\tilde{F}_1 + l_z^2\left(3\sigma_\parallel - \sigma_\perp\right) + \sigma_\perp - v_M^2\right] < 0, \tag{53}$$

or

$$l_z\sqrt{\tilde{F}_1 + 3\sigma_\parallel} < v_M < \sqrt{\tilde{F}_1 + \sigma_\perp + l_z^2(3\sigma_\parallel - \sigma_\perp)}. \tag{54}$$

where $\tilde{F}_n = \partial_n F^{-1}(n)$. One can easily see that no soliton is possible for purely parallel propagation i.e. $l_z = 1$. For purely perpendicular propagation ($l_z = 0$), the condition reduces to,

$$v_M < \sqrt{\tilde{F}_1 + \sigma_\perp}. \tag{55}$$

For isotropic ion pressure, condition (54) reduces to [11],

$$l_z\sqrt{\tilde{F}_1 + \sigma} < v_M < \sqrt{\tilde{F}_1 + \sigma}. \tag{56}$$

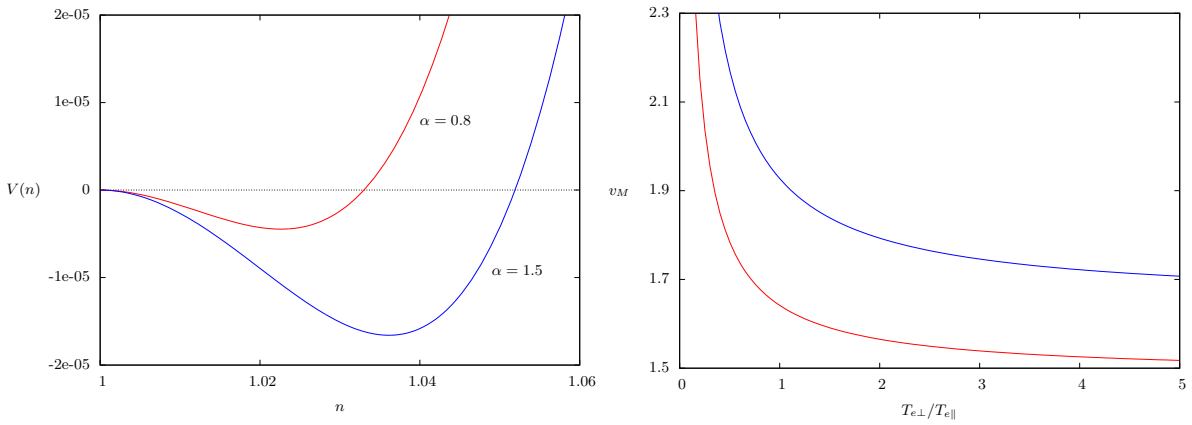

Figure 2. The dependence of pseudo potential structure (left) and limiting Mach number (right) on the electron thermal anisotropy parameter α. Note that $\alpha > 1$ signifies negative anisotropy ($T_{e\perp} > T_{e\parallel}$). While for large negative anisotropy the limiting Mach number reaches a constant value, for large positive anisotropy, the Mach number may reach high values. The ion anisotropy parameters are $\sigma_\parallel = 1.5, \sigma_\perp = 1.0$ [36].

Naturally, this can severely alter the energy regime where a solitary structure can form as the Mach number actually indicates the total energy being pumped into a solitary structure. In Fig.1, we show these two limits for the Mach number.

5.2. Effect of electron thermal anisotropy

We note that the effect of electron thermal anisotropy is related to the magnetic field line variation within the soliton through the anisotropy factor $\gamma(\phi)$, which is parameterised by the field line ratio $B_0/B_s(\phi)$. This justification for this demands an explanation.

The plasma approximation we have used in this work essentially means that the Debye shielding length is at least a few orders of magnitude smaller than the size of the nonlinear structures, which is found to be correct for the parameter regime of magnetospheric plasmas. This also ignores the small scale variation of the ambient magnetic field within the soliton width. In order to model the magnetic field variation within the soliton width, we consider a state *far away* from a relaxed plasma state i.e. the state of Taylor relaxation [43], so that in the moving frame of the soliton, we can write [44],

$$\boldsymbol{E} \simeq \eta \boldsymbol{j}, \tag{57}$$

which helps us in estimating the electrostatic potential ϕ,

$$\phi \sim -\eta \int j_\parallel \, dl \sim -\eta \frac{BL}{\mu_0 l} + \text{const.}, \tag{58}$$

where the plasma resistivity can be thought to be a result of field line stochasticity within the solitary structure. The scale length l is the width of the electric current structure and L is the length over which the integration is carried out.

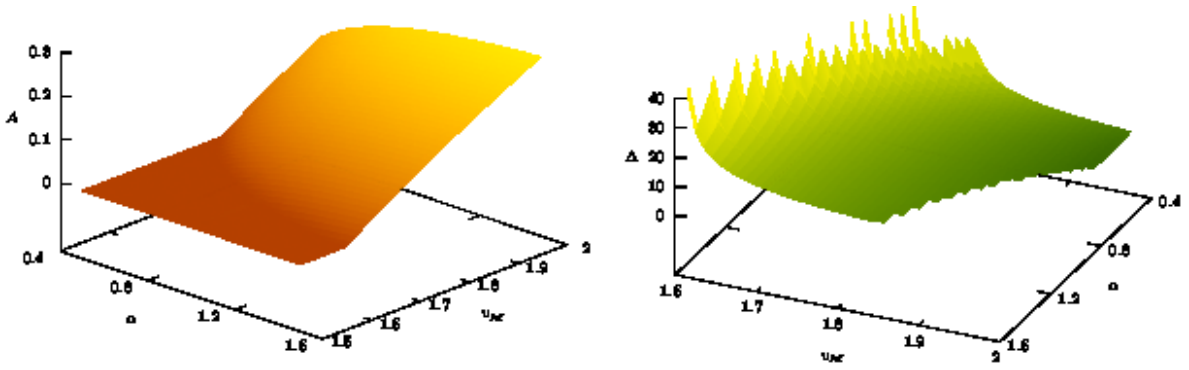

Figure 3. The dependence of soliton amplitude A (left) and width Δ (right) with the electron temperature anisotropy and Mach number.

We now note that the electron density is given by Eqs.(45,46). Though we have chosen to parameterise the dependence of magnetic field line B_s on the plasma potential as per the relation (58), we note that the resultant equation for n_e i.e. Eq.(45) becomes analytically non-invertible in terms of ϕ. So, we approximate Eq.(58) for small ϕ as,

$$\frac{B_s}{B_0} \sim e^{-\phi}. \tag{59}$$

which also reduces to the correct asymptotic value at the limit $\phi \to 0$ in conformation with relation (58). The plasma potential is now given by,

$$\phi = \ln\left(\frac{n\alpha}{1-n+n\alpha}\right), \tag{60}$$

where $\alpha = T_{e\perp}/T_{e\parallel}$ is a measure of electron temperature anisotropy. With this, the bounds on limiting Mach number becomes,

$$l_z\left(\frac{1}{\alpha}+3\sigma_\parallel\right)^{1/2} < v_M < \left[\frac{1}{\alpha}+l_z^2(3\sigma_\parallel-\sigma_\perp)+\sigma_\perp\right]^{1/2} \tag{61}$$

which becomes

$$\left.\begin{aligned} l_z\left(3\sigma_\parallel\right)^{1/2} < \;\; v_M \;\; < \left[l_z^2(3\sigma_\parallel-\sigma_\perp)+\sigma_\perp\right]^{1/2}, \qquad & \alpha \gg 1, \\ l_z\alpha^{-1/2} < \;\; v_M \;\; < \alpha^{-1/2}, \qquad & \alpha \ll 1. \end{aligned}\right\} \tag{62}$$

A pseudo potential formation and the dependence of the limiting Mach number on the thermal anisotropy parameter α, are shown in Fig.2. As we can see that for large α (large negative anisotropy), the allowed Mach number interval becomes constant, whereas for small α (large positive anisotropy), the interval becomes progressively narrower with Mach number reaching a very high value. If we analyse the soliton amplitude and width, we observe that soliton amplitude A increases with α and Mach number and the width decreases with Mach number while it is largely independent on α. Physically we expect to see large amplitude and slow moving soliton in the region of large negative anisotropy. The dependence of soliton amplitude A and width Δ with the anisotropy parameter and Mach number are shown in Fig.3.

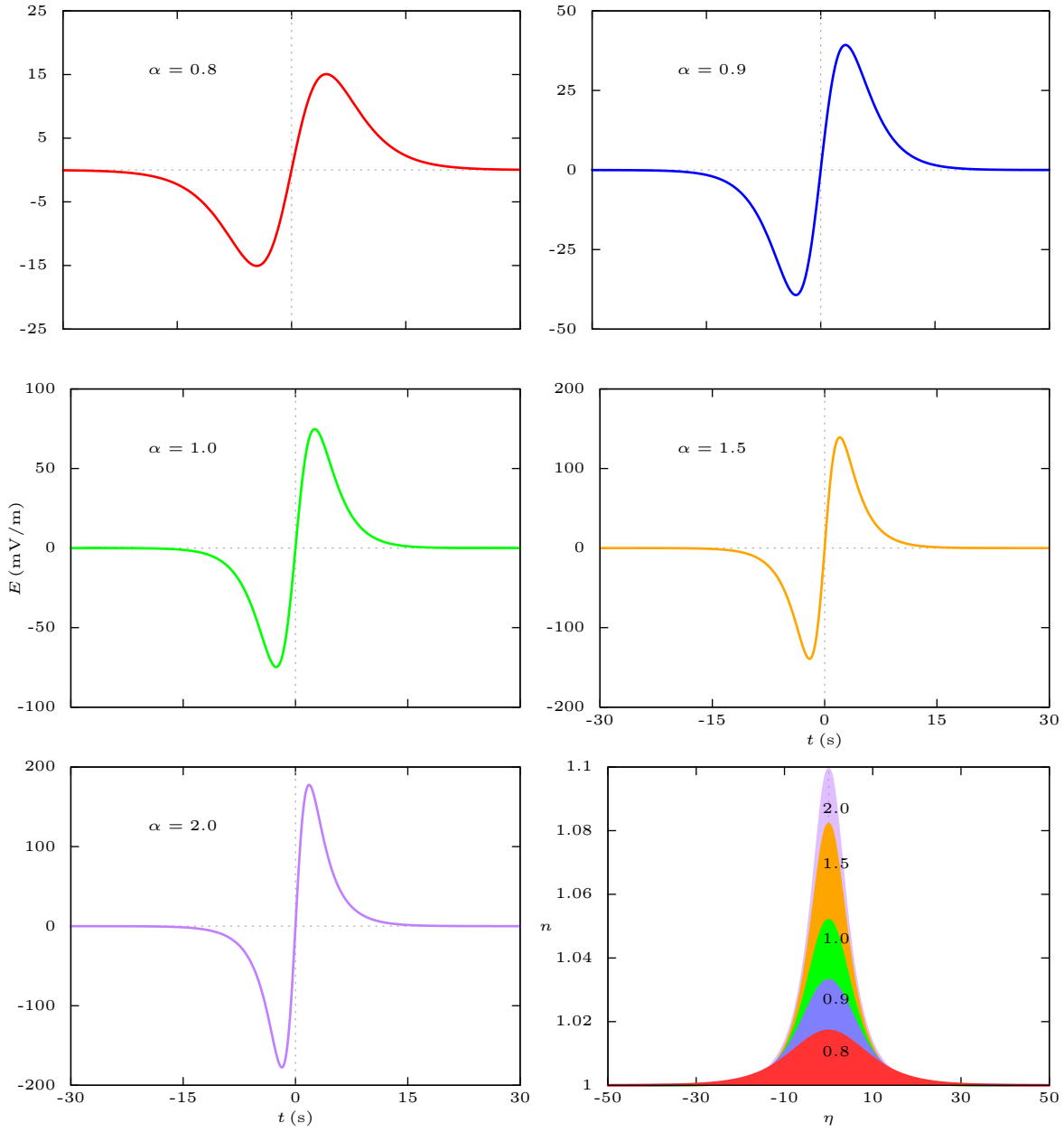

Figure 4. Bipolar electric field structures, in the rest frame of the detector, show as they vary in size with respect to the electron thermal anisotropy parameter α. The bottom right panel shows the corresponding density solitons. The embedded numbers represent corresponding values of α. The ion anisotropy parameters are $\sigma_{\parallel} = 1.5, \sigma_{\perp} = 1.0$ [36].

Note that the soliton amplitude A is given by first zero of the pseudo potential away from $n = 1$. The width Δ is related to the maximum depth d of the soliton as $\Delta = A/\sqrt{d}$. The shallower is the potential, the narrower is the soliton.

6. Comparison with experimental data

In this section, we try to interpret certain experimental results. However, our results should only indicate an overall trend in the observational data rather than definitively reproducing experimental results. A major contribution to our knowledge about temporally and spatially localised electrostatic structures in the auroral regions are due to the Freja and FAST satellite missions in the 90's. These satellite missions clearly demonstrated the existence of such structures [45]. More recently, observations by Cluster spacecrafts at a geocentric distance of about $\sim 5R_E$ gave a good idea about detailed parameters of these structures [46]. Some typical parameters of these localised structures are peak-to-peak electric field variations of about $\sim 30 - 170\,\mathrm{mV/m}$ with a life time ranging from $10 - 280\,\mathrm{secs}$ [46]. Note that the nonlinear structures observed in these near-earth plasmas actually fall into the ion-acoustic time scale which also includes the Alfvén time scale and this has been confirmed by various experimental data as well as theoretical works [47].

On the other hand there are strong evidences of electron thermal anisotropy in the auroral regions, which are due to several satellite based investigations viz. IMP 6 [48], AMPTE/CCE [49], AMPTE/IRM, [50] and SCATHA [35]. Typically, electron thermal anisotropy is present almost all throughout across the range of electron energies $\sim 0.1 - 10\,\mathrm{keV}$. In most cases, a positive anisotropy ($T_{e\|} > T_{e\perp}$) is observed in lower energies up to $\sim 1\,\mathrm{keV}$ and negative anisotropy ($T_{e\|} < T_{e\perp}$) is observed toward the higher electron energy $\sim 10\,\mathrm{keV}$ [36]. In order to compare these results, we transform the density soliton to a bipolar electric field structure, which is what detected on board these satellites. From the relation (60), we can find out the equivalent electric field as,

$$E = -\frac{d\phi}{d\eta} = -\frac{1}{[n + (\alpha - 1)n^2]}\frac{dn}{d\eta}. \tag{63}$$

Note that for the electron anisotropy parameter $\alpha = 1$ (isotropic), the relation reduces to the classical Boltzmannian relation. The width of these structures can be transformed to rest frame of the satellite in terms of pulse duration, as reported experimentally. With the normalisation we have used, we now plot these bipolar structures for various values of electron thermal anisotropy along with the soliton structures in Fig.4. In our calculations, we have assumed an average electron temperature of $\sim 10\,\mathrm{keV}$, which is typical for these parameters of negative anisotropy ($\alpha > 1.0$) in these regions [36]. The Mach number is fixed at 1.7 for which we get the width of these structure in the rest frame of the detector in the order of $\sim 30\,\mathrm{s}$ (in terms of pulse life-time). These numbers largely agree with observed data in the auroral regions as reported by these satellite based observations. As we can see from Fig.4 that as the electron anisotropy parameter increases, the peak-to-peak variation of the electric field becomes more, we

can conclude that the electron thermal anisotropy has a decisive role in determining the amplitude of these electrostatic structure. However, we still do not have direct observational data about these electrostatic structures in auroral plasmas measured in relation to the electron thermal anisotropy.

7. Summary and conclusions

In this work, we have analysed the formation of electrostatic solitary structures through a pseudo potential analysis in a magnetoplasma with both electron and ion anisotropy which is induced by the ambient magnetic field along with a weak collisional regime. The ion thermal anisotropy is modelled through a CGL double adiabatic equations of state while the electron anisotropy is incorporated with a bi-Maxwellian distribution. In the ion-acoustic time scale, the electrons are considered inertia-less. We have shown that a self-consistent inclusion of both ion and electron thermal anisotropies can possibly explain large amplitude electrostatic structures observed in the region of negative electron thermal anisotropy in the magnetosphere.

However, we note that the CGL double adiabatic theory has only very limited application in a restricted parameter regime. Nevertheless, it does show us in principle, the effect of ion thermal anisotropy. It also calls for a more comprehensive analysis which involves realistic pressure anisotropy such as polybaric equations of state [30].

Acknowledgement

One of the authors, MK acknowledges UGC for fellowship grant (RFSMS). The authors would like to thank two anonymous referees for making the work more informative.

References

[1] Moola S, Bharuthram R, Singh S V and Lakhina G S 2003 *Pramana* **61** 1209
[2] Matsumoto H, Kojima H, Omura Y, Okada M, Nagano I and Tsutsui 1994 *Gephys. Res. Lett.* **21** 2915
[3] Franz J R, Kintner P M and Pichett J S 1998 *Geophys. Res. Lett.* **25** 1277
[4] Ergun R E et al. 1998 *Geophys. Res. Lett.* **25** 2041
[5] Picket J S et al. 2008 *Adv. Space Res.* **41** 1666
[6] Tsurutani B T, Arballo J K, Lakhina G S, Ho C M, Buti B, Pickett J S and Gurnett D A 1998 *Geophys. Res. Lett.* **25** 4117
[7] Lakhina G S, Tsurutani B T, Kojima H and Matsumoto H 2000 *J. Geophys. Res.* **105** 27791
[8] Franz J R, Kintner P M, Pickett J S and Chen L-J 2005 *J. Geophys. Res.* **110** A09211
[9] Williams J D, Chen L-J, Kurth W S, Gurnett D A, Dougherty M K and Rymer A M 2005 *Geophys. Res. Lett.* **32** L17103
[10] Bora M P, Choudhury B and Das G C 2012 *Astrophys. Space Sci.* **341** 515
[11] Choudhury B, Goswami R, Das G C and Bora M P 2013 *Phys. Plasmas* **20** 042902
[12] Blanc M, Kallenbach R and Erkaev N V 2005 *Space Sci. Rev.* **116** 227
[13] Schekochihin A A, Cowley S C, Kulsrud R M and Sharma P 2005 *ApJ* **629** 139
[14] Seough J, Yoon P H, Kim K-H and Lee D-H 2013 *Phys. Rev. Lett.***110** 071103
[15] Sharp R D, Shelley E G, Johnson R G and Ghielmetti A G 1980 *J. Geophys. Res.* **85** 92

[16] Collin H L, Sharp R D and Shelley E G 1982 *J. Geophys. Res.* **87** 7504
[17] Meuris P and Verheest F 1996 *Phys. Lett. A* **219** 2992
[18] Adnan M, Williams G, Qamar A, Mahmood S and Kourakis I 2014 *Eur. Phys. J. D* **68** 247
[19] Choi C R, Ryu C-M, Lee D-Y, Lee N C and Kim Y-H 2007 *Phys. Lett. A* **364** 297
[20] Choi C R, Ryu C-M, Lee N C, Lee D-Y and Kim Y-H 2005 *Phys. Plasmas* **12** 07231
[21] Adnan M, Mahmood S and Qamar A 2014 *Contrib. Plasma Phys.***54** 724
[22] Adnan M, Mahmood S and Qamar A 2014 *Adv. Space Res.***53** 845
[23] Chuang S-H, Hau L-N 2009 *Phys. Plasmas* **16** 022901
[24] Chew G F, Goldberger M L and Low F E 112 *Proc. R. Soc. A* **236** 112
[25] Carlson C W, McFadden J P, Ergun R E et al. 1998 *Geophys. Res. Lett.* **25** 2017
[26] McFadden J P et al. 1998 *Geophys. Res. Lett.* **25** 2025
[27] Ergun E R, Su Y J, Anderson L et al. *Phys. Rev. Lett.* **87** 045003
[28] Anderson L, Ergun R E, Main D et al. 2002 *Phys. Plasmas* **9** 3600
[29] Kulsrud R M 1982 *Handbook of Plasma Physics (Eds M N Rosenbluth and R Z Sagdeev), North-Holland 115*
[30] Stasiewicz K 2005 *Phys. Rev. Lett.***95** 015004
[31] Stasiewicz K 2004 *Gephys. Res. Lett.***31** L21 804
[32] Stasiewicz 2004 *Phys. Rev. Lett.* **93** 125004
[33] Schulz M and Eviatar A 1973 *J. Geophys. Res.***78** 3948
[34] Olsen R C 1981 *J. Geophys. Res.***86** 11235
[35] Richardson J D, Fennell J F and Croley Jr D R 1981 *J. Geophys. Res.* **86** 10105
[36] Janhunen P, Olsson A, Laakso H and Vaivads A 2004 *Ann. Geophys.* **22** 237
[37] Whipple Jr E C 1977 *J. Geophys. Res.* **82** 1525
[38] Moncuquet M, Bagenal F and Meyer-Vernet N 2002 *J. Geophys. Res.* **107** SMP 24-1
[39] Huang T S and Birmingham T J 1992 *J. Geophys. Res.* **97** 1511
[40] Marghitu O, Klecker B and McFadden J P 2006 *Adv. Space Res.***38** 1694
[41] Janhunen P and Olsson A 2008 *Ann. Geophysicae* **16** 292
[42] Štverák Š, Trávníček P, Maksimovic M, Marsch E, Fazakerley A N and Scime E E 2008 *J. Geophys. Res.***113** A03103
[43] Taylor J B 1974 *Phys. Rev. Lett.* **33** 1139
[44] Wilmot-Smith A L, Hornig G and Pontin D I 2009 *ApJ* **696** 1339
[45] Marklund G, Blomberg L, Flthammar C-G, Lindqvist P-A and Eliasson L 1995 *Ann. Geophysicae* **13** 704
[46] Marklund G T et al. 2004 *Nonlin. Processes Geophys.* **11** 709
[47] Ekeberg J, Wannberg G, Eliasson L and Stasiewicz K 2010 *Ann. Geophys.***28** 1299
[48] Hada T, Nishida A, Terasawa T and Hones Jr E W 1981 *J. Geophys. Res.* **86** 11211
[49] Klumpar D M, Quinn J M and Shelley E G 1988 *J. Geophys. Res.* **93** 1295
[50] Sergeev V A, Baumjohann W and Shiokawa K 2001 *Geophys. Res. Lett.* **28** 3813